DMD Fast Forward. Published on January 13, 2006 as doi:10.1124/dmd.105.007740
This article has not been copyedited and formatted. The final version may differ from this version.

DMD #7740

Mutational analysis of polar amino acid residues within predicted transmembrane helices 10 and 16 of Multidrug Resistance Protein 1 (ABCC1): Effect on substrate specificity

Da-Wei Zhang[1], Kenichi Nunoya[2], Monika Vasa, Hong-Mei Gu, Susan P. C. Cole, and Roger G. Deeley

From the Division of Cancer Biology and Genetics, Cancer Research Institute (D.W.Z., K.N., M.V., S.P.C.C., R.G.D.), Departments of Pathology & Molecular Medicine(S.P.C.C., R.G.D.), Biochemistry (R.G.D.)and Anatomy & Cell Biology (H.M.G.), Queen's University, Kingston, Ontario K7L 3N6, Canada

Running Title: Mutational and functional analysis of wild type and mutant human MRP1

Corresponding author:

Roger G. Deeley

Cancer Research Institute, Suite 300, 10 Stuart St. Kingston, Ontario K7L 3N6, Canada. Tel.: 613-533-2979; Fax: 613-533-6830; E-mail: deeleyr@post.queensu.ca

Text pages: 28

Tables: 1

Figures: 7

References: 34

Words in the Abstract: 247

Words in the Introduction: 627

Words in the Discussion: 1413

Abbreviations: MDR, multidrug resistance; MRP, Multidrug resistance protein; P-gp, P-glycoprotein; CFTR, cystic fibrosis transmembrane conductance regulator; MSD, membrane-spanning domain; TM, transmembrane; NBD, nucleotide binding domain; ICD, intracellular domain; mAb, monoclonal antibody; $E_2$17βG**,** 17β-estradiol 17-(β-D-glucuronide); LTC_4, leukotriene C_4; MTT, 3-(4,5-dimethylthiazol-2-yl)-2,5-diphenyltetrazolium bromide; DOX, doxorubicin; VCR, vincristine; VP-16, etoposide; SDS-PAGE, sodium dodecyl sulfate-polyacrylamide gel electrophoresis; HEK, human embryonic kidney; PBS, phosphate-buffered saline.

ABSTRACT

Human Multidrug Resistance Protein1 (MRP1) has a total of 17 transmembrane (TM) helices arranged in three domains, MSD0, MSD1 and MSD2 with a 5+6+6 TM configuration. Photolabeling studies indicate that TMs 10 and 11 in MSD1 and 16 and 17 in MSD2 contribute to the substrate binding pocket of the protein. Previous mutational analyses of charged and polar amino acids in predicted TM helices 11, 16 and 17 support this suggestion. Mutation of Trp^{553} in TM10 also affects substrate specificity. To extend this analysis, we mutated six additional polar residues within TM10 and the remaining uncharacterized polar residue in TM16, Asn^{1208}. Although mutation of Asn^{1208} was without effect, two of six mutations in TM10, T550A and T556A modulated the drug resistance profile of MRP1 without affecting transport of leukotriene C4, estradiol-17β-D-glucuronide ($E_2$17βG) and glutathione. Mutation T550A increased vincristine resistance but decreased doxorubicin resistance, while mutation T556A decreased resistance to VP-16 and doxorubicin. Although conservative mutation of Tyr^{568} in TM10 to Phe or Trp had no apparent effect on substrate specificity, substitution with Ala decreased the affinity of MRP1 for $E_2$17βG without affecting drug resistance or the transport of other substrates tested. These analyses confirm that several amino acids in TM10 selectively alter the substrate specificity of MRP1 suggesting that they interact directly with certain substrates. The location of these and other functionally important residues in TM helices 11, 16 and 17 is discussed in the context of an energy-minimized model of the membrane spanning domains of MRP1.

INTRODUCTION

Human multidrug resistance protein1 (MRP1) is a member of the 'C' branch of the ATP-binding cassette transporter (ABC) superfamily and has been designated ABCC1. The predicted topology of MRP1 consists of a typical P-glycoprotein (P-gp)-like core region, composed of two membrane spanning domains (MSDs 1and 2), each with six transmembrane (TM) α-helices, and two nucleotide binding domains (NBDs). In addition, MRP1 contains an NH_2-terminal MSD, MSD0, which consists of five TMs with an extracellular NH_2-terminus (Hipfner et al., 1997; Bakos et al., 1996; Kast et al., 1997). Thus the protein contains three MSDs with a total of 17 predicted TM helices (5+6+6, Figure 1).

MRP1 confers resistance to many commonly used natural product chemotherapeutic agents including anthracyclines, *Vinca* alkaloids, and epipodophyllotoxins, as well as methotrexate and certain heavy metal oxyanions (Cole et al., 1992; Cole et al., 1994). However, transport of unmodified drugs by MRP1 is both GSH and ATP dependent (Renes et al., 1999; Loe et al., 1998; Rappa et al., 1997). In some cases, GSH appears to be co-transported with these compounds (Renes et al., 1999; Loe et al., 1998; Rappa et al., 1997). Detailed *in vitro* transport measurements using MRP1-enriched inside-out membrane vesicles have demonstrated that MRP1 is capable of directly transporting many glutathione-, glucuronide-, and sulfate-conjugated organic anion conjugates, such as the glutathione conjugate cysteinyl leukotriene 4 (LTC_4), and glucuronate conjugate 17β-estradiol 17-(β-D-glucuronide) ($E_2$17βG) in an ATP-dependent manner (Loe et al., 1996a; Loe et al., 1996b; Muller et al., 1994; Jedlitschky et al., 1996; Leier et al., 1996; Mao et al., 2000). The mechanism by which MRP1 binds and transports such structurally unrelated cytotoxic drugs and conjugated organic anions remains an active area of study. In the absence of a crystal structure of the protein, identification of amino acid residues

involved in determining substrate specificity and transport activity, coupled with structural predictions, has provided valuable insights into the mechanism by which MRP1 recognizes structurally diverse compounds.

Photoaffinity labeling studies have implicated TMs -10, -11, -16 and -17 of MRP1 as components of the substrate binding pocket(s) of the protein (Qian et al., 2001; Daoud et al., 2001; Qian et al., 2002; Mao et al., 2002). Previously, we have demonstrated that certain amino acid residues with hydrogen bonding side chains located in the putative TM11 and -17 of MRP1 are important, either for overall activity or substrate specificity of the protein (Haimeur et al., 2002; Koike et al., 2002; Zhang et al., 2001a; Zhang et al., 2002; Zhang et al., 2001b; Ito et al., 2001; Zhang et al., 2004; Haimeur et al., 2004). Trp^{553} and Pro^{557}, located within TM10 of MRP1, have also been shown to be important for the transport activity of the protein (Koike et al., 2002; Koike et al., 2004). More recently, charged residues Arg^{1197}, Arg^{1202} and Glu^{1204}, and the polar residue Trp^{1198}, predicted to be within TM16, have been reported to be essential for function (Koike et al., 2004; Situ et al., 2004). We have now examined the role of additional residues with hydrogen bonding capability within TM10 and -16. In TM10, Thr^{550}, Thr^{552}, Thr^{556}, Thr^{564} and Thr^{570} were individually mutated to Ala, and Tyr^{568} was mutated to Ala, Ser, Phe and Trp. Asn^{1208} within TM16 was replaced by Ala. These mutant proteins were then stably expressed in human embryonic kidney (HEK293) cells, and the transfectants were characterized with respect to their drug resistance profiles, as wells as their ability to transport LTC_4, $E_2$17βG and GSH. Mutation N1208A in TM16 had no detectable effect on the function of MRP1. However, two polar residues, Thr^{550} and Thr^{556} located in TM10 play an important role in determining the drug resistance profile, and the aromatic side chain of the residue at position 568 of TM10 of MRP1 is important for $E_2$17βG transport.

Materials and Methods

Materials

Culture medium and fetal bovine serum were obtained from Life Technologies, Inc. [^{3}H]LTC$_4$ (38 Ci/mmol) was purchased from Amersham Pharmacia Biotech and [^{3}H]E$_2$17βG (44 Ci/mmol) and [^{3}H]GSH from PerkinElmer Life Sciences. Doxorubicin HCl, etoposide (VP-16), and vincristine sulfate were obtained from Sigma.

Site-directed Mutagenesis

Mutation T564A was generated using the Transformer^{TM}Site-Directed Mutagenesis kit (CLONTECH, Palo Alto, CA). Templates were prepared as described previously (Zhang et al., 2004). Mutagenesis was then performed according to the manufacturer's instructions using a selection primer 5'-GAG AGT GCA CGA TAT CCG GTG TG-3' that mutates a unique NdeI site in the vector to an EcoRV restriction site. An oligonucleotide bearing the mismatched base at the residue to be mutated (underlined) was synthesized by ACGT Corp. (Toronto, Canada) with the following sequence: 5'- G GTG GCC TTG TGC GCA TTT GCC GTC TAC-3'. Mutations T550A, T552A, T556A, Y568A, Y568S, Y568F, Y568W, T570A, and N1208A were generated using the Quikchange^{TM}Site-Directed Mutagenesis kit (STRATAGENE, La Jolla, CA). Mutagenesis was then performed according to the manufacturer's instructions. Oligonucleotides bearing mismatched bases at the residues to be mutated (underlined) were synthesized by ACGT Corp. (Toronto, Canada) with the following sequences: T550A (5'-G TCA GCC GTG GGC GCC TTC ACC TGG GT-3'), T552A (5'-C GTG GGC ACC TTC GCC TGG GTC TGC AC-3'),

T556A (5'-C ACC TGG GTC TGC GCG CCC TTT CTG GT-3'), Y568A (5'-TGC ACA TTT GCC GTC GCC GTG ACC ATT GAC GA-3'), Y568S (5'-TGC ACA TTT GCC GTC TCC GTG ACC ATT GAC GA-3'), Y568F (5'-TGC ACA TTT GCC GTC TTC GTG ACC ATT GAC GA-3'), Y568W (5'-TGC ACA TTT GCC GTC TGG GTG ACC ATT GAC GA-3'), T570A (5'-T GCC GTC TAC GTG GCC ATT GAC GAG AAC AAC-3'), N1208A (5'-GCC GTG CGG CTG GAG TGT GTG GGC GCC-3').

After confirming all mutations by DNA sequencing (ACGT Corp., Toronto, Canada), DNA fragments containing the desired mutations were transferred into pCEBV7-MRP1. After reconstructing full-length expression vectors containing the mutations, the integrity of the mutated inserts and cloning sites was verified by DNA sequencing (ACGT Corp., Toronto, Canada).

Cell lines and Tissue Culture

Stable transfection of HEK293 cells with the pCEBV7 vector containing the wild type and mutant MRP1 cDNAs has been described previously (Zhang et al., 2001a). Briefly, HEK293 cells were transfected with pCEBV7 vectors containing mutant MRP1 using Fugene6 (Roche Molecular Biochemicals) according to the manufacturer's instructions. After ~48 h, the transfected cells were supplemented with fresh medium containing 100 μg/ml hygromycin B. Approximately 3 weeks after transfection, the hygromycin B-resistant cells were cloned by limiting dilution and the resulting cell lines were tested for high level expression of the mutant proteins.

Determination of Protein Levels in Transfected Cells

Plasma membrane vesicles were prepared by centrifugation through sucrose, as described previously (Loe et al., 1996a; Zhang et al., 2001a). After determination of protein levels by Bradford assay (Bio-Rad), total membrane protein (0.5 μg, 1.0 μg, and 1.25 μg) from transfectants expressing wild type MRP1 and various mutant proteins were resolved on a 7.5% sodium dodecyl sulfate-polyacrylamide gel electrophoresis (SDS-PAGE) and then transferred onto Immobilon-P polyvinylidene difluoride membranes (Millipore, Bedford, MA). The proteins were detected with mAb, MRPm6 (Alexis Biochemicals, San Diego, CA) and the signal was enhanced using Renaissance chemiluminescence reagent (PerkinElmer Life Sciences). Relative levels of MRP1 expression were determined by densitometry of exposed films.

Confocal Microscopy

Confocal microscopy was carried out as described previously (Zhang et al., 2001a, Zhang et al., 2001b). Briefly, ~$5x10^5$ stably-transfected HEK293 cells were seeded in each well of a 6-well tissue culture dish on coverslips. When the cells had grown to confluence, they were washed once in PBS and then fixed with 2% paraformaldehyde in PBS, followed by permeabilization using digitonin (0.25 mg/ml in PBS). MRP1 proteins were detected with the monoclonal antibody MRPm6. Antibody binding was detected with Alexa Fluor 488 anti-mouse IgG (H+L) $(Fab')_2$ fragment. Nuclei were stained with propidium iodide. Localization of MRP1 in the transfected cells was determined using a Meridian Insight confocal microscope (filter, 620/40 nm for propidium iodide; 530/30 nm for Fluor 488).

LTC_4, $E_2$17βG and GSH Transport by Membrane Vesicles

DMD Fast Forward. Published on January 13, 2006 as DOI: 10.1124/dmd.105.007740
This article has not been copyedited and formatted. The final version may differ from this version.

Plasma membrane vesicles were prepared as described previously, and ATP-dependent transport of [^{3}H]LTC_4 into the inside-out membrane vesicles was measured by a rapid filtration technique (Loe et al., 1996a; Zhang et al., 2001a). Briefly, vesicles (10 μg protein) were incubated at 23°C in 100 μl of transport buffer (50 mM Tris-HCl, 250 mM sucrose, 0.02% sodium azide, pH7.4) containing ATP or AMP (4 mM), 10 mM $MgCl_2$ and [^{3}H]LTC_4 (50 nM, 200 nCi). At the indicated times, 20 μl aliquots were removed and added to 1 ml of ice-cold transport buffer, followed by filtration under vacuum through glass fiber filters (Type A/E, Gelman Sciences, Dorval, Quebec, Canada). Filters were immediately washed twice with 4 ml of cold transport buffer. The bound radioactivity was determined by scintillation counting. All data were corrected for the amount of [^{3}H]LTC_4 that remained bound to the filter in the absence of vesicle protein (usually <5% of the total radioactivity). [^{3}H]LTC_4 uptake was expressed relative to the total protein concentration in each reaction. ATP-dependent uptake of [^{3}H]$E_2$17βG (400 nM, 120 nCi) was measured as described for [^{3}H]LTC_4 except that the temperature used was 37˚C.

K_m and V_{max} values of ATP-dependent [^{3}H]LTC_4 uptake by membrane vesicles (2.5 μg protein) were measured at various LTC_4 concentrations (0.01 to 1 μM) for 1 min at 23˚C in 25 μl of transport buffer containing 4 mM ATP and 10 mM $MgCl_2$, followed by linear transformation using a Hanes-Woolf plot. Kinetic parameters of ATP-dependent [^{3}H]$E_2$17βG (0.1-16 μM) uptake were determined as described for [^{3}H]LTC_4 except that the temperature used was 37˚C.

GSH uptake was also measured by rapid filtration with membrane vesicles (20 μg of protein) incubated at 37 °C for 20 min in a 60-μl reaction volume with [^{3}H]GSH (100 μM, 300 nCi) in the absence and presence of verapamil (100μM). To minimize GSH catabolism by γ-

glutamyltranspeptidase during transport, membranes were preincubated in 0.5 mM acivicin for 10 min at 37 °C prior to measuring [^{3}H]GSH uptake in the presence of verapamil (100 μM).

Chemosensitivity Testing

Drug resistance was determined using the colorimetric 3-(4,5-dimethylthiazol-2-yl)-2,5-diphenyl tetrazolium bromide (MTT) assay as described previously (Cole et al., 1994; Zhang et al., 2001a). Mean values of quadruplicate determinations (±S.D.) were plotted using GraphPad software. IC_{50} values were obtained from the best fit of the data to a sigmoidal curve. Relative resistance is expressed as the ratio of the IC_{50} value of cells transfected with MRP1 expression vectors compared with cells transfected with empty vector. Resistance was determined in three or more independent experiments.

DMD Fast Forward. Published on January 13, 2006 as DOI: 10.1124/dmd.105.007740
This article has not been copyedited and formatted. The final version may differ from this version.

RESULTS

Expression of mutant MRP1 in stably transfected HEK293 cells—Thr^{550}, Thr^{552}, Thr^{556}, Thr^{564}, Tyr^{568}, and Thr^{570} within TM10, and Asn^{1208} within TM16 were replaced individually by Ala (Fig. 1). The episomal expression vector, pCEBV7, containing mutated forms of MRP1 cDNAs was used to stably transfect HEK293 cells and populations of transfected cells were selected in hygromycin B. The resultant stably-transfected cell populations were cloned by limiting dilution and subpopulations expressing high levels of MRP1 mutant proteins were used in subsequent studies. The levels of mutant proteins relative to wild type MRP1 in previously characterized HEK transfectants were determined by immunoblotting and densitometry (Fig. 2A). The expression levels of these mutant proteins in stably transfected HEK293 cells ranged from 50 to 90% of wild-type MRP1. Endogenous MRP1 in HEK293 cells transfected with the empty vector was undetectable under the conditions used (data not shown).

To determine whether these mutations influenced trafficking of the protein, we compared the subcellular localization of wild-type and mutant MRP1 by confocal microscopy. The subcellular distribution of the mutated proteins assessed by immunoreactivity with the MRP1 specific mAb MRPm6 was indistinguishable from that of cells expressing wild type protein (Fig. 2B). In all cases, strong plasma membrane staining was observed, indicating that trafficking was unaffected.

Transport of [^{3}H]LTC_4 and [^{3}H]$E_2$17βG by wild type and mutant MRP1—To determine whether any of the mutations altered the efficiency with which the protein transported LTC_4 and $E_2$17βG, we examined ATP-dependent uptake of these compounds by membrane vesicles prepared from HEK transfectants expressing each of the mutant proteins (Fig. 3). The levels of LTC_4 uptake by vesicles prepared from HEK transfectants expressing either wild type or mutant

MRP1 were proportional to the relative expression levels of the wild type and mutant proteins (Fig. 3A to 3C). Thus, these polar residues may not be involved in the binding and transport of LTC_4. ATP-dependent transport of [^{3}H]$E_2$17βG was also examined (Fig. 3D to 3F), only replacement of Tyr^{568} with Ala decreased the transport efficiency by approximately 60%, indicating that the polar and/or the bulky aromatic side chain of the residue at position 568 is important for the ability of MRP1 to transport $E_2$17βG.

*Effect of mutations Y568S, Y568F, Y568W on the transport of [^{3}H]LTC_4 and [^{3}H]$E_2$17βG by MRP1*— Since replacement of Tyr^{568} by Ala selectively decreased transport of $E_2$17βG, this residue was also mutated to Ser, Phe and Trp. These three mutations were then stably expressed in HEK293 cells. Immunoblotting indicated that the expression levels of mutant MRP1^{Y568F}, MRP1^{Y568S}, and MRP1^{Y568W} were 90, 50 and 90% of wild-type MRP1, respectively (Fig. 4A). The effects of these mutations on the ability of MRP1 to transport LTC_4 and $E_2$17βG were then examined (Fig. 4B and 4C). Like mutation Y568A, substitution of Tyr^{568} with Ser did not affect the transport of LTC_4 but decreased $E_2$17βG transport. However, replacement of Tyr^{568} with the more conservative residues, Phe and Trp, had no effect on transport of either compound (Fig. 4B and 4C). Thus the aromaticity or steric bulk of the residue at position 568, but not the side chain polarity, plays a role in determining the efficiency of transporting the conjugated estrogen.

Kinetic parameters of [^{3}H]LTC_4 and [^{3}H]$E_2$17βG transport by wild type and Y568A mutant MRP1—To more precisely determine the influence of mutation Y568A on the ability of MRP1 to transport $E_2$17βG, we compared kinetic parameters for the wild type and mutant proteins (Fig. 5). For wild type MRP1 and Y568A, the K_m and normalized V_{max} values for LTC_4 uptake were essentially identical. Linear regression using a Hanes-Woolf transformation yielded values of 115 nM and 143 nM, and 76.8 pmol/mg/min and 64 pmol/mg/min, for the K_m and V_{max}

values of wild-type and Y568A proteins, respectively (Fig. 5B and 5C). For $E_2$17βG transport, a comparable analysis yielded K_m values of 1.4 μM and 5.4 μM and normalized V_{max} values of 170 pmol/mg/min and 190 pmol/mg/min for wild-type and mutant proteins, respectively (Fig. 5D and 5E). Thus, mutation of Tyr^{568} appears to decrease the affinity of MRP1 for $E_2$17βG approximately 4-fold without affecting its transport capacity.

Resistance profiles of wild type and mutant human proteins—The drug resistance profiles of transfectants expressing mutant proteins were determined using MTT assays. The results are presented as relative drug resistance factors in Table 1. Mutation of Asn^{1208} in TM16 had no effect on the ability of MRP1 to confer resistance to any of the three classes of drugs tested. However, mutation of two Thr residues in TM10 altered the drug resistance profile (Table 1). Substitution T550A reduced resistance to doxorubicin approximately 2-fold and increased resistance to vincristine approximately 4.5 fold, but had no effect on VP-16 resistance. In contrast, mutation T556A reduced the resistance to both VP-16 and doxorubicin approximately 2-fold without affecting vincristine resistance. Thus, elimination of the polarity of the side chains of residues at positions 550 and 556 differentially affects the drug resistance profile of MRP1 suggesting that these two Thr residues may interact directly with drug substrates.

Transport of [^{3}H]GSH by wild type and mutant MRP1—We have shown that mutations T550A and T556A all affect the ability of MRP1 to confer drug resistance, whereas mutation Y568A only influenced the transport of $E_2$17βG. One major distinction between MRP1-mediated transport of substrates such as LTC_4 and $E_2$17βG, and drugs such as vincristine and daunorubicin, is a requirement for GSH, which may be co-transported with the unmodified drug (Renes et al., 1997; Loe et al., 1998; Rappa et al., 1997; Mao et al., 2000). Previously, we have reported that MRP1 exhibits low levels of ATP-dependent GSH transport that can be dramatically stimulated

by verapamil (Loe et al., 2000). Thus, we examined the effects of mutations made in TM10 and -16 on verapamil-stimulated GSH transport by MRP1 to determine whether any mutations that affected drug resistance also influenced the GSH transport (Fig. 6). As observed with the effects of the mutations on LTC_4 transport, none of these mutations had any significant effect on verapamil-stimulated GSH transport, consistent with the suggestion that they modify interactions between MRP1 and the drug rather than an altering of the ability to bind and transport GSH.

Discussion

Photolabeling studies indicate that amino acids in predicted TM helices 10, 11,16 and 17 are probable components of the substrate binding pocket of MRP1 (Qian et al., 2001; Daoud et al., 2001; Mao et al., 2002). Mutational studies have also shown that a number of polar amino acids in TM helices 11, 16 and 17 are major determinants of substrate specificity and overall transport activity of the protein (Haimeur et al., 2002; Koike et al., 2002; Zhang et al., 2001a; Zhang et al., 2002; Zhang et al., 2001b; Ito et al., 2001; Zhang et al.; 2004; Haimeur et al., 2004). The majority of the functionally important polar residues in TM11 and TM17 are in the predicted inner leaflet region of the membrane (Zhang et al., 2002; Zhang et al., 2001b; Ito et al., 2001; Zhang et al.; 2004; Haimeur et al., 2004; Situ et al., 2004). Mapping of these residues on to an energy minimized model of the tertiary structure of MSD1 and MSD2 of MRP1 suggests that most of their side chains project towards, or line, a central cavity presumed to be the translocation pathway of the protein (Campbell et al., 2004). Thus they are available to interact with substrate or the side chains of amino acids in neighboring TM helices (Fig. 7). To provide additional experimental evidence for or against the proposed structure, we have extended the mutational analysis to polar residues in TM10 and mutated the remaining uncharacterized polar residue in TM16.

The predicted outer leaflet region of TM16 is devoid of polar amino acids (Figure 1B) and mutation of the vicinal cysteine residues, Cys^{1205} and Cys^{1209}, was found previously to have no effect on substrate specificity or overall activity (Olsen et al., 1998). Similarly, mutation of Arg^{1202} had no effect on transport activity of MRP1. On the other hand, replacement of Glu^{1204} with Leu or Arg^{1197} with Glu or Lys affected either substrate specificity or overall transport activity of MRP1 (Situ et al., 2004). Mutation of Trp^{1198} to Ala also dramatically decreased

overall transport activity (Koike et al., 2002). Based on the model shown (Fig. 7), these amino acids and several other functionally important residues in TM17, cluster in the predicted inner leaflet region of the two TMs with their side chains projecting towards TMs 10 and 11. The remaining polar residue in TM16, Asn^{1208}, is also predicted to project into the translocation pore (Fig.7). However, mutation of Asn^{1208} had no effect on transport or drug resistance. Similarly, mutation of two polar residues in TM17, $Ser^{1235}$and Gln^{1237}, with side chains predicted to project into the pore also had no effect (Fig.7) (Zhang et al., 2002). In all cases, these residues are located towards the outer leaflet of the membrane relative to the cluster of amino acids that affect substrate specificity or overall activity.

Mutation of Trp^{553} and Pro^{557} in TM10 alters the overall transport activity of MRP1 rather than substrate specificity (Koike et al., 2002; Koike et al., 2004). To further examine the role of amino acids in TM10, we mutated five Thr residues and Tyr^{568}. Mutations of Thr^{552}, Thr^{564}, and Thr^{570} had no effect on either the drug resistance profile or organic anion transport activity. Thr^{552} is predicted to be in the inner leaflet region of the membrane, but its side chain projects away from the predicted pore. As found with polar residues in TMs11, 12, 16 and 17 of MRP1 that do not affect substrate specificity, Thr^{564} and Thr^{570} are predicted to be located in the outer leaflet region of TM10. Similarly, conservative mutation of Tyr^{568}, which is also predicted to be in the outer leaflet, to either Phe or Trp had no effect on substrate specificity. However, non-conservative mutation to Ala or Ser selectively decreased transport of $E_2$17βG without affecting the transport of LTC_4 or GSH, or resistance to any drug tested. Mutation of two of the five Thr residues, Thr^{550} and Thr^{556}, differentially affected drug resistance without altering transport of organic anion conjugates tested. Thr^{550} and Thr^{556} are predicted to be in the inner leaflet region of TM10 and the side chains of both residues align with that of Trp^{553}. Taken

together, these findings confirm the role of TM10 in determining substrate specificity and overall transport activity of MRP1.

We have previously proposed that hydrogen-bonding may be a common form of interaction between MRP1 and its substrates (Zhang et al., 2001a; Zhang et al., 2002; Zhang et al., 2001b; Ito et al., 2001; Zhang et al., 2003a; Zhang et al., 2003b). The differential effect of eliminating the hydrogen bonding potential of Thr^{550} and Thr^{556} on drug resistance supports this suggestion. However, since the transport of vincristine and doxorubicin by MRP1 is GSH dependent, we also examined the possibility that these mutations might influence interaction of MRP1 with GSH rather than drug (Loe et al., 1998; Renes et al., 1999). However, the Thr^{550} and Thr^{556} mutations had no effect on basal or verapamil stimulated GSH transport (Loe et al., 2000). Overall, the effects of these two mutations suggest that Thr^{550} and Thr^{556} may form hydrogen bonds with some drug substrates, such as doxorubicin and VP-16. The increase in resistance to vincristine observed with the T550A mutation may be attributable to the smaller size of the Ala side chain that favors transport of the larger drug. Similar behavior was observed following Ala mutations of Asn^{597} and Asn^{1245} in TM11 and TM17, respectively (Zhang et al., 2002; Zhang et al., 2004). Like the T550A mutation, these mutations decreased resistance to VP-16 and increased resistance to vincristine.

Thr^{550}, Thr^{556} and the previously identified Trp^{553} in TM10 together with Phe^{594} in TM11 are predicted to be in the inner leaflet region and to project towards functionally important residues in TM17 (Fig.7). Two of these residues, Trp^{1246} and Tyr^{1243} , together with Trp^{553} and Phe^{594} have been postulated to form part of an aromatic basket at the cytoplasmic entrance to the translocation pathway (Koike et al., 2002; Zhang et al., 2002; Ito et al., 2001; Campbell et al., 2004). Similar clusters of functionally important aromatic and polar amino acids are present in

DMD Fast Forward. Published on January 13, 2006 as DOI: 10.1124/dmd.105.007740
This article has not been copyedited and formatted. The final version may differ from this version.

the inner leaflet regions of TM11 and TM16 (Fig.7). Although mutation of residues in these clusters has been shown to selectively affect the ability of MRP1 to confer resistance to various drugs and to transport $E_2$17βG, only mutations of Phe^{594} differentially affected transport of substrates including LTC_4 (Campbell et al., 2004). Despite the cross-linking of LTC_4 to regions spanning these helices, amino acids important for specific interaction with this substrate appear to belocated in other TM helices, including TMs 6, 9 and 15 (Haimeur et al., 2002; Haimeur et al., 2004).

The predicted location of Tyr^{568} close to the extracellular/membrane interface distinguishes it from other polar residues in TM10 and the polar residues in TMs 11, 16 and 17 that influence substrate specificity. Many of the conjugated substrates of MRP1 are relatively hydrophilic and it appears likely that they interact with the protein from the cytosol rather than by diffusion through the membrane. Consequently, the predicted location of Tyr^{568} at the distal end of the translocation pathway raised the possibility that it might be involved in a step in the transport of $E_2$17βG subsequent to initial binding, such as substrate translocation and release. However, kinetic analysis showed that the non-conservative mutation Y568A increased the apparent K_m for $E_2$17βG approximately 5-fold, without altering V_{max}. Thus the mutation appears to affect a step that we are presently unable to distinguish kinetically from substrate binding. The side chain of Tyr^{568} is predicted to be within 2Å of Pro^{343} in TM6, mutation of which results in a major decrease in transport of $E_2$17βG and to a lesser extent, the transport of other substrates (Koike et al., 2004). Based on our current model of MRP1, the longest distance between side chains of residues in TM17 close to the cytosol/membrane interface that influence transport and those in the outer leaflet of TM6 and TM10 is approximately 22Å. This is approximately equivalent to the longest dimension of $E_2$17βG. Thus it is feasible that binding of at least some

substrates may involve contacts that span both lipid bilayers. However, since binding of some substrates by MRP1 appears to cause conformational changes in the membrane spanning domains (Manciu et al., 2003), it is also possible that the interaction with residues such as Pro^{343} Tyr^{568} may occur subsequent to a conformational change triggered by initial docking of $E_2$17βG with residues in the inner leaflet region of the protein.

Acknowledgements – The authors wish to thank Derek Shulze for advice on confocal microscopy.

References

Bakos E, Hegedus T, Hollo Z, Welker E, Tusnady GE, Zaman GJ, Flens MJ, Varadi A and Sarkadi B (1996) Membrane topology and glycosylation of the human multidrug resistance-associated protein. *J Biol. Chem.* **271:** 12322-12326.

Campbell JD, Koike K, Moreau C, Sansom MS, Deeley RG and Cole SPC (2004) Molecular modeling correctly predicts the functional importance of Phe594 in transmembrane helix 11 of the multidrug resistance protein, MRP1 (ABCC1). *J. Biol. Chem.* **279:** 463-468.

Cole SPC, Bhardwaj G, Gerlach JH, Mackie JE, Grant CE, Almquist KC, Stewart AJ, Kurz EU, Duncan AM and Deeley RG (1992) Overexpression of a transporter gene in a multidrug-resistant human lung cancer cell line. *Science* **258:** 1650-1654.

Cole SPC, Sparks KE, Fraser K, Loe DW, Grant CE, Wilson GM and Deeley RG (1994) Pharmacological characterization of multidrug resistant MRP-transfected human tumor cells. *Cancer Res.* **54:** 5902-5910.

Daoud R, Julien M, Gros P and Georges E (2001) Major photoaffinity drug binding sites in multidrug resistance protein 1 (MRP1) are within transmembrane domains 10-11 and 16-17. *J Biol. Chem.* **276:** 12324-12330.

Haimeur A, Deeley RG and Cole SPC (2002) Charged amino acids in the sixth transmembrane helix of multidrug resistance protein 1 (MRP1/ABCC1) are critical determinants of transport activity. *J Biol. Chem.* **277:** 41326-41333.

Haimeur A, Conseil G, Deeley RG and Cole SPC (2004) Mutations of charged amino acids in or near the transmembrane helices of the second membrane spanning domain differentially affect the substrate specificity and transport activity of the multidrug resistance protein MRP1 (ABCC1). *Mol. Pharmacol.* **65:** 1375-1385.

Hipfner DR, Almquist KC, Leslie EM, Gerlach JH, Grant CE, Deeley RG and Cole SPC (1997) Membrane topology of the multidrug resistance protein (MRP). A study of glycosylation-site mutants reveals an extracytosolic NH2 terminus. *J Biol. Chem.* **272:** 23623-23630.

Ito K, Olsen SL, Qiu W, Deeley RG and Cole SPC (2001) Mutation of a single conserved tryptophan in multidrug resistance protein 1 (MRP1/ABCC1) results in loss of drug resistance and selective loss of organic anion transport. *J Biol. Chem.* **276:** 15616-15624.

Jedlitschky G, Leier I, Buchholz U, Barnouin K, Kurz G and Keppler D (1996) Transport of glutathione, glucuronate, and sulfate conjugates by the MRP gene-encoded conjugate export pump. *Cancer Res.* **56:** 988-994.

Kast C and Gros P (1997) Topology mapping of the amino-terminal half of multidrug resistance-associated protein by epitope insertion and immunofluorescence. *J Biol. Chem.* **272:** 26479-26487.

Koike K, Oleschuk CJ, Haimeur A, Olsen SL, Deeley RG and Cole SPC (2002) Multiple membrane-associated tryptophan residues contribute to the transport activity and substrate specificity of the human multidrug resistance protein, MRP1. *J. Biol. Chem.* **277:** 49495-49503.

Koike K, Conseil G, Leslie HE, Deeley RG, and Cole SPC (2004) Identification of proline residues in the core cytoplasmic and transmembrane regions of multidrug resistance protein 1 (MRP1/ABCC1) important for transport function, substrate specificity, and nucleotide interactions. *J. Biol. Chem.* **279:** 12325-12336.

Loe DW, Almquist KC, Deeley RG and Cole SPC (1996a) Multidrug resistance protein (MRP)-mediated transport of leukotriene C4 and chemotherapeutic agents in membrane vesicles. Demonstration of glutathione-dependent vincristine transport. *J Biol. Chem.* **271:** 9675-9682.

Loe DW, Almquist KC, Cole SPC and Deeley RG (1996b) ATP-dependent 17 beta-estradiol 17-(beta-D-glucuronide) transport by multidrug resistance protein (MRP). Inhibition by cholestatic steroids. *J Biol. Chem.* **271:** 9683-9689.

Loe DW, Deeley RG and Cole SPC (1998) Characterization of vincristine transport by the M(r) 190,000 multidrug resistance protein (MRP): evidence for cotransport with reduced glutathione. *Cancer Res.* **58:** 5130-5136.

Loe DW, Deeley RG and Cole SPC (2000) Verapamil stimulates glutathione transport by the 190-kDa multidrug resistance protein 1 (MRP1). *J Pharmacol. Exp. Ther.* **293:** 530-538.

Loo TW, Bartlett MC and Clarke DM (2004) Disulfide cross-linking analysis shows that transmembrane segments 5 and 8 of human P-glycoprotein are close together on the cytoplasmic side of the membrane. *J. Biol. Chem.* **279:** 7692-7697.

Lugo MR and Sharom FJ (2005) Interaction of LDS-751 with P-glycoprotein and mapping of the location of the R drug binding site. *Biochemistry* **441:** 643-655.

Manciu L, Chang XB, Buyse F, Hou YX, Gustot A, Riordan J R, and Ruysschaert JM (2003) Intermediate structural states involved in MRP1-mediated drug transport. Role of glutathione. *J Biol. Chem.* **278:** 3347-3356.

Mao Q, Qiu W, Weigl KE, Lander PA, Tabas LB, Shephard RL, Dantzig AH, Deeley RG and Cole SPC (2002) GSH-dependent photolabeling of multidrug resistance protein MRP1 (ABCC1) by [125I]LY475776. Evidence of a major binding site in the COOH-proximal membrane spanning domain. *J Biol. Chem.* **277:** 28690-28699.

Muller M, Meijer C, Zaman GJ, Borst P, Scheper RJ, Mulder NH, de Vries EG and Jansen PL (1994) Overexpression of the gene encoding the multidrug resistance-associated protein results in increased ATP-dependent glutathione S-conjugate transport. *Proc. Natl. Acad. Sci U. S. A.* **91:** 13033-13037.

Olsen SL, Leslie EM, Loe DW, Ooi AL-J, Deeley RG and Cole SPC (1998) Site-directed mutagenesis of vicinal cysteine residues in human multidrug resistance protein, MRP. *Proc. Amer. Assoc. Cancer Res.* **39:** 1145.

Qian YM, Qiu W, Gao M, Westlake CJ, Cole SPC and Deeley RG (2001) Characterization of binding of leukotriene C4 by human multidrug resistance protein 1: evidence of differential interactions with NH2- and COOH-proximal halves of the protein. *J Biol. Chem.* **276:** 38636-38644.

Qian YM, Grant CE, Westlake CJ, Zhang DW, Lander PA, Shepard RL, Dantzig AH, Cole SPC and Deeley RG (2002) Photolabeling of human and murine multidrug resistance protein 1 with the high affinity inhibitor [125I]LY475776 and azidophenacyl-[35S]glutathione. *J Biol. Chem.* **277:** 35225-35231.

Rappa G, Lorico A, Flavell RA and Sartorelli AC (1997) Evidence that the multidrug resistance protein (MRP) functions as a co-transporter of glutathione and natural product toxins. *Cancer Res.* **57:** 5232-5237.

Renes J, de Vries EG, Nienhuis EF, Jansen PL and Muller M (1999) ATP- and glutathione-dependent transport of chemotherapeutic drugs by the multidrug resistance protein MRP1. *Br. J Pharmacol.* **126:** 681-688.

Situ D, Haimeur A, Conseil G, Sparks KE, Zhang D, Deeley RG, and Cole SPC (2004) Mutational analysis of ionizable residues proximal to the cytoplasmic interface of membrane spanning domain 3 of the multidrug resistance protein, MRP1 (ABCC1): glutamate 1204 is important for both the expression and catalytic activity of the transporter. *J. Biol. Chem.* **279:** 38871-38880.

Zhang DW, Cole SPC and Deeley RG (2001a) Identification of an amino acid residue in multidrug resistance protein 1 critical for conferring resistance to anthracyclines. *J Biol. Chem.* **276:** 13231-13239.

Zhang DW, Cole SPC and Deeley RG (2001b) Identification of a nonconserved amino acid residue in multidrug resistance protein 1 important for determining substrate specificity: evidence for functional interaction between transmembrane helices 14 and 17. *J Biol. Chem.* **276:** 34966-34974.

Zhang DW, Cole SPC and Deeley RG (2002) Determinants of the substrate specificity of multidrug resistance protein 1: role of amino acid residues with hydrogen bonding potential in predicted transmembrane helix 17. *J Biol. Chem.* **277:** 20934-20941.

Zhang DW, Gu HM, Situ D, Haimeur A, Cole SPC and Deeley RG (2003a) Functional importance of polar and charged amino acid residues in transmembrane helix 14 of multidrug resistance protein 1 (MRP1/ABCC1): identification of an aspartate residue critical for conversion from a high to low affinity substrate binding state. *J. Biol. Chem.* **278:** 46052-46063.

Zhang DW, Gu HM, Vasa M, Muredda M, Cole SPC and Deeley RG (2003b) Characterization of the role of polar amino acid residues within predicted transmembrane helix 17 in determining the substrate specificity of multidrug resistance protein 3. *Biochemistry* **42:** 9989-10000.

Zhang DW, Nunoya K, Vasa M, Gu HM, Theis A, Cole SPC and Deeley RG (2004) Transmembrane helix 11 of multidrug resistance protein 1 (MRP1/ABCC1): identification of polar amino acids important for substrate specificity and binding of ATP at nucleotide binding domain 1. *Biochemistry* **43:** 9413-9425.

Footnotes:

This work was supported by a grant from the National Cancer Institute of Canada with funds from the Terry Fox Run

Da-Wei Zhang and Kenichi Nunoya contributed equally to this work

[1]current address: Howard Hughes Medical Institute and Department of molecular genetics, University of Texas Southwestern Medical Center at Dallas, 5323 Harry Hines Blvd., Dallas, TX 75390, USA.

[2]current address: Department of Xenobiotic Metabolism and Disposition, Minase Research Institute, Ono Pharmaceutical Co., Ltd, 3-1-1 Sakurai Shimamoto-cho, Mishima-gun, Osaka 618-8585, Japan

Figure Legends

FIG. 1. Topology of human MRP1. *Panel A*: the predicted topology of human MRP1 with 17 transmembrane (TM) helices. The putative TM10 and -16 are indicated by lighter shading. *Panel B*: an expanded view of TM10 and -16. Mutated polar residues are indicated by *shaded circles.*

FIG. 2. Expression of mutant MRP1 in stably transfected HEK293 cells. *Panel A:* Expression levels of wild type and mutant MRP1 proteins in membrane vesicles isolated from stably transfected HEK293 cells were determined by immunobloting of membrane vesicle preparations and densitometry as described. Blots were probed with the MRP1-specific mAb MRPm6. The numbers below the blot refer to the levels of the mutant MRP1 proteins relative to the levels of wild type MRP1 proteins in membrane vesicles prepared from the stably transfected HEK293 cells. Values are mean of 3 independent experiments. *Panel B:* The subcellular localization of wild type and mutant MRP1 was determined by confocal microscopy as described. MRP1 was detected using mAb MRPm6. Location of MRP1 is indicated in green. Nuclei were stained with propidium iodide and are shown in red. Transfectants tested were expressing wild type or mutant MRP1 as indicated in the figure. An x-y optical section of the cells is shown to illustrate the distribution of the wild type and mutant proteins between plasma and intracellular membranes.

FIG. 3. ATP-dependent [^{3}H]LTC_4 and $E_2$17βG uptake by membrane vesicles prepared from HEK293 cells stably transfected with wild type or mutant MRP1. *Panel A to C*:ATP-dependent [^{3}H]LTC_4 uptake. Briefly, membrane vesicles were incubated at 23°C with 50 nM LTC_4 (200 nCi) in transport buffer for the time indicated, as described. *Panel D to F:* ATP-

DMD Fast Forward. Published on January 13, 2006 as DOI: 10.1124/dmd.105.007740
This article has not been copyedited and formatted. The final version may differ from this version.

dependent uptake of [^{3}H]$E_2$17βG. Briefly, membrane vesicles were incubated at 37 °C with 400 nM [^{3}H]$E_2$17βG (120 nCi) in transport buffer for the time indicated, as described. Transfectants tested were: $HEKpc_7$(■), HEK_{MRP1}(▲), $HEK_{MRP1T550A}$(▼), $HEK_{MRP1T552A}$(♦), $HEK_{MRP1T556A}$(●), $HEK_{MRP1T564A}$(□), $HEK_{MRP1Y568A}$(Δ), $HEK_{MRP1T570A}$(∇), and $HEK_{MRP1N1208A}$(◊). The uptake of LTC_4 and $E_2$17βG by membrane vesicles prepared from control and wild type MRP1-transfected HEK293 cells in transport buffer containing 4 mM AMP was also examined and shown in *Panel A and D* [$HEKpc_7$(○), and HEK_{MRP1}(+)].Data shown have been normalized to compensate for differences in the relative expression levels of the wild type and mutant proteins. Values are mean ± S.D. of ≥ 3 independent experiments.

FIG. 4. ATP-dependent [^{3}H]LTC_4 and [^{3}H]$E_2$17βG uptake by membrane vesicles prepared from HEK293 cells transfected with wild type or mutant MRP1. *Panel A*: Expression levels of wild type and mutant MRP1 proteins in membrane vesicles isolated from stably transfected HEK293 cells were determined by immunobloting of membrane vesicle preparations and densitometry as described in the legend to Figure 2A. [^{3}H]LTC_4 (*Panel B*) and [^{3}H]$E_2$17βG (*Panel C*) uptake by wild type and mutant proteins was determined as described in the legends to Figure 3. The normalized transport values were obtained by adjusting experimentally determined values (1 min time point) to compensate for differences in the relative levels of the wild type and mutant proteins. Values are mean ± S.D. of ≥ 3 independent experiments.

FIG. 5. Kinetics of ATP-dependent [^{3}H]LTC_4 and [^{3}H]$E_2$17βG uptake. *Panel A*: Expression levels of wild type and mutant MRP1 proteins in membrane vesicles isolated from transiently

transfected HEK293 cells were determined by immunobloting of membrane vesicle preparations and densitometry as described in the legend to Figure 2A. The numbers below the blot refer to the levels of mutant MRP1 proteins relative to the levels of wild type MRP1 protein in membrane vesicles prepared from the stably transfected HEK293 cells. *Panel B and C:* The initial rate of ATP-dependent [^{3}H]LTC_4 uptake by membrane vesicles prepared from HEK293 cells transfected with wild type or mutant proteins was measured at various LTC_4 concentrations (0.01 to 1 μM) for 1 min at 23 ºC as described. *Panel D and E:* [^{3}H]$E_2$17βG uptake was determined as described for [^{3}H]LTC_4 except that the reactions were carried out at 37 ºC with various concentrations of $E_2$17βG (0.1 to 16 μM). Values are mean ± S.D. of triplicate determinations in a single experiment. Similar results were obtained from one more experiment. *Panel B and D*: Data were plotted as V_0 versus [S] to confirm that the concentration range selected was appropriate to observe both zero-order and first-order rate kinetics. *Panel C and E*: Data were plotted as [S]/V versus [S]. The transfectants tested were: HEK_{MRP1}(■), and $HEK_{MRP1Y568A}$(▲). Kinetics parameters for LTC_4 and $E_2$17βG transport were determined from non-linear and linear regression analysis of the combined data. Details of K_m and V_{max} values for wild type and mutant MRP1 are provided under "Results."

FIG. 6. ATP-dependent verapamil-stimulated [^{3}H]GSH uptake by membrane vesicles prepared from HEK293 cells stably transfected with wild type or mutant MRP1. Membrane vesicles were incubated at 37 °C with 100 μM GSH (300 nCi) in transport buffer in the presence of verapamil (100 μM) as described. Transfectants tested expressed wild type or mutant MRP1 as indicated in the figures. The normalized transport values were obtained by adjusting

experimentally determined values (20 min time point) to compensate for differences in the relative levels of the wild type and mutant proteins and are shown in *Panel B*. Data shown in *panel A* have not been normalized to compensate for differences in expression levels. Values are mean ± S.D. of 3 independent experiments.

FIG. 7. Energy minimized model of MRP1 TM's 10, 11, 16 and 17

Panel A: The figure shows TMs 10, 11, 16 and 17 viewed in the plane of the membrane (top) or from the extracellular face (bottom). The predicted membrane interfaces are indicated by broken lines in the left-hand panel. The energy-minimized model is based on the structure of the lipid A transporter from *Vibrio cholera*, VC-Msba. The derivation of this model of MSD1 and MSD2 of MRP1 has been described in detail in Campbell *et al.* (Campbell et al., 2004). For clarity, other TMs in these two MSDs have been removed and the side chains of only selected residues have been shown using PyMol. Previously mutated residues in TMs 10, 16 and 17 that do or do not influence substrate specificity or overall activity are shown in red and blue, respectively. Residues in TM10 which when mutated alter substrate specificity or overall activity include: Thr^{550}, Thr^{556} and Thr^{564} (green), Trp^{553} (yellow), Pro^{557} (violet) and Tyr^{568} (orange). The residue in TM17 indicated by the arrow is Arg^{1249}, the side chain of which is approximately 7.5Å from the side chain of Trp^{553}. *Panel B*: A schematic of TM10 and TM16 with mutated polar residues referred to in the text indicated by *shaded circles*.

DMD Fast Forward. Published on January 13, 2006 as DOI: 10.1124/dmd.105.007740
This article has not been copyedited and formatted. The final version may differ from this version.

TABLE 1

Relative drug resistance of HEK293 cells transfected with wild type and mutant MRP1

The resistance of HEK293 cells transfected with expression vectors encoding wild type and mutant MRP1 relative to that of cells transfected with empty vector were determined using a tetrazolium salt-based microtiter plate assay. The relative resistance factor was obtained by dividing the IC_{50} values for wild type/mutant MRP1-transfected cells by the IC_{50} value for control transfectants. The values shown represent the mean standard deviation (± S.D.) of relative resistance values determined from 3 independent experiments. Resistance factors normalized for differences in the levels of mutant proteins expressed in the transfectant populations used are shown in parentheses.

Transfectant	Drug (Relative Resistance Factor)		
	Vincristine	VP-16	Doxorubicin
HEK_{MRP1}	36.0 ± 7.5 (36.0)	12.5 ± 2.7 (12.5)	9.6 ± 0.9 (9.6)
$HEK_{MRP1T550A}$	144.9 ± 27.3 (161.0)	12.4 ± 2.3 (13.8)	3.9 ± 0.3 (4.3)
$HEK_{MRP1T552A}$	21.6 ± 3.5 (36.0)	7.5 ± 1.6 (12.5)	5.5 ± 2.1 (9.2)
$HEK_{MRP1T556A}$	25.0 ± 6.8 (41.6)	3.4 ± 1.4 (5.6)	2.5 ± 1.3 (4.1)
$HEK_{MRP1T564A}$	12.1 ± 2.6 (24.2)	5.7 ± 2.8 (11.4)	4.3 ± 0.8 (8.6)
$HEK_{MRP1Y568A}$	33.4 ± 4.9 (41.7)	11.3 ± 2.4 (14.1)	7.9 ± 1.9 (9.9)
$HEK_{MRP1T570A}$	32.0 ± 2.4 (40.0)	10.4 ± 1.8 (13.0)	7.2 ± 0.9 (9.0)
$HEK_{MRP1N1208A}$	25.6 ± 2.3 (32.0)	14.7 ± 1.8 (18.3)	8.8 ± 2.4 (11.0)
$HEK_{MRP1Y568S}$	16.2 ± 0.9 (32.4)	6.8 ± 0.9 (13.6)	5.1 ± 0.4 (10.2)
$HEK_{MRP1Y568F}$	28.9 ± 3.5 (32.1)	9.8 ± 1.7 (10.9)	8.3 ± 0.4 (9.2)
$HEK_{MRP1Y568W}$	30.2 ± 2.7 (33.6)	9.6 ± 2.3 (10.7)	9.2 ± 2.5 (10.2)

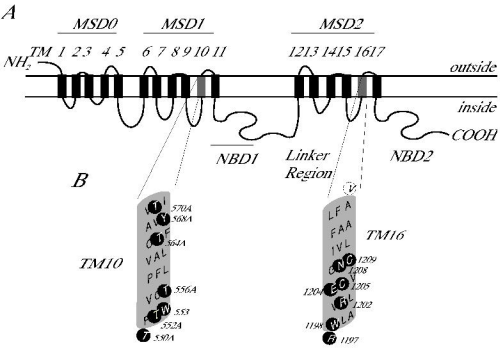
A
MSD0
MSD1
MSD2
NH2
TM 1 2 3 4 5
6 7 8 9 10 11
12 13 14 15 16 17
outside
inside
COOH
NBD1
Linker Region
NBD2
B
TM10
TM16

Figure 1

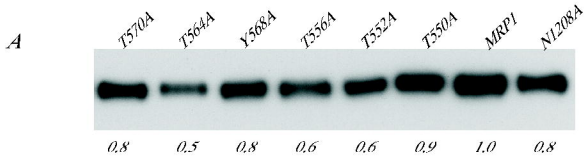
A
T570A
T564A
Y568A
T556A
T552A
T550A
MRP1
N1208A
0,8
0,5
0,8
0,6
0,6
0,9
1,0
0,8

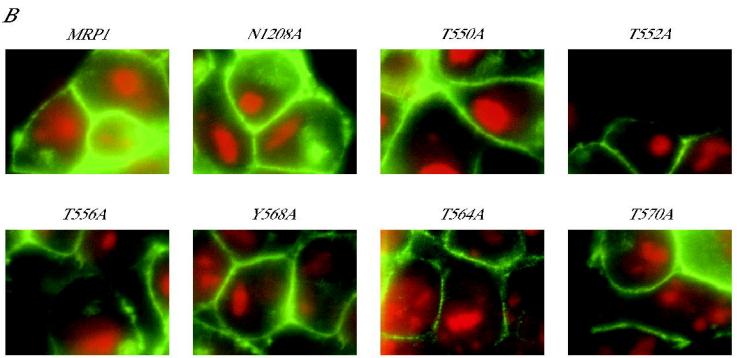
B
MRP1
N1208A
T550A
T552A
T556A
Y568A
T564A
T570A

Figure 2

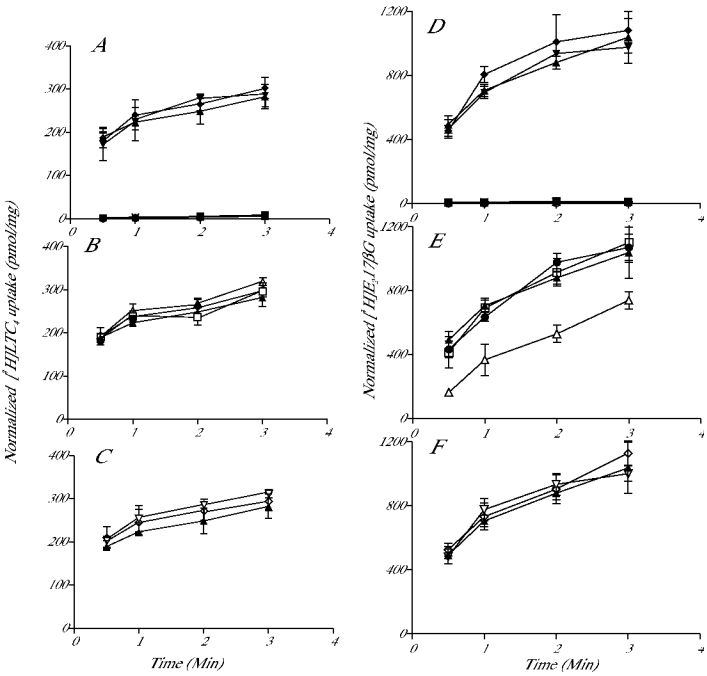
A
B
C
D
E
F
Normalized [³H]LTC₄ uptake (pmol/mg)
Normalized [³H]E₂17βG uptake (pmol/mg)
Time (Min)
Time (Min)

Figure 3

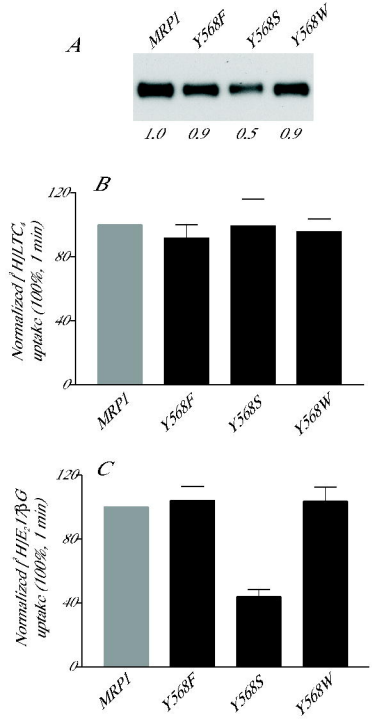
A
MRP1
Y568F
Y568S
Y568W
1.0
0.9
0.5
0.9
B
Normalized [3H]LTC4 uptake (100%, 1 min)
120
80
40
0
MRP1
Y568F
Y568S
Y568W
C
Normalized [3H]E217βG uptake (100%, 1 min)
120
80
40
0
MRP1
Y568F
Y568S
Y568W

Figure 4

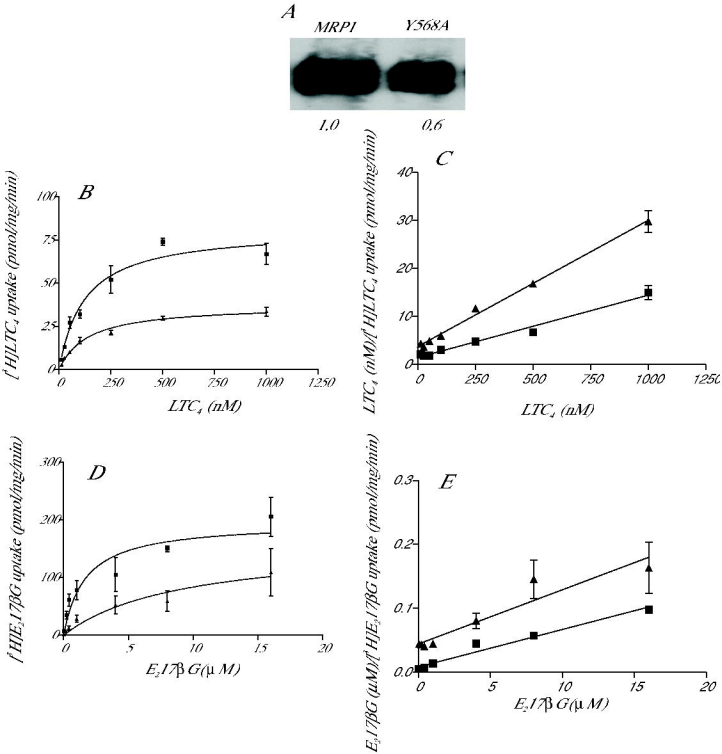
A
MRP1
Y568A
1,0
0,6
B
[³H]LTC₄ uptake (pmol/mg/min)
LTC₄ (nM)
C
LTC₄ (nM)/[³H]LTC₄ uptake (pmol/mg/min)
LTC₄ (nM)
D
[³H]E₂17βG uptake (pmol/mg/min)
E₂17β G(μ M)
E
E₂17βG (μM)/[³H]E₂17βG uptake (pmol/mg/min)
E₂17β G(μ M)

Figure5

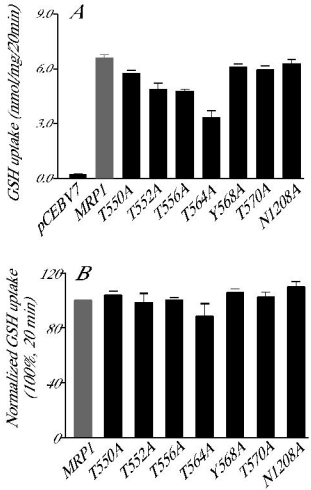
A
GSH uptake (nmol/mg/20min)
9.0
6.0
3.0
0.0
pCEBV7
MRP1
T550A
T552A
T556A
T564A
Y568A
T570A
N1208A
B
Normalized GSH uptake (100%, 20 min)
120
80
40
0
MRP1
T550A
T552A
T556A
T564A
Y568A
T570A
N1208A

Figure 6

A

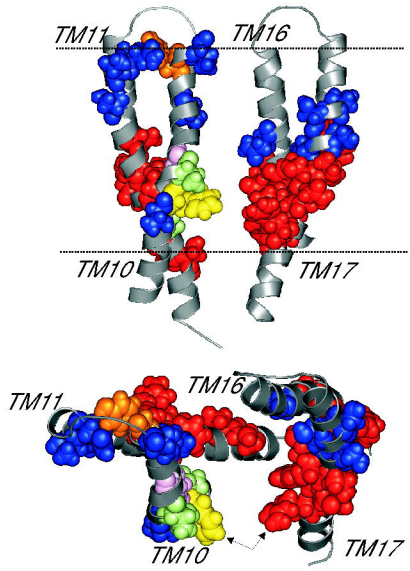
TM11
TM16
TM10
TM17
TM11
TM16
TM10
TM17

B

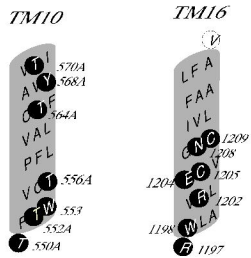
TM10
TM16
570A
568A
564A
556A
553
552A
550A
1209
1208
1205
1204
1202
1198
1197

Figure 7